EXPERIMENTAL ANALYSIS ON LANDING DYNAMICS OF MARTIAN MOON SPACECRAFT BASED ON SIMILARITY LAW

*Daiki Yamaguchi[1], Genya Ishigami[2]

[1]*Keio University, Yokohama, Japan, E-mail: daikiyamaguchi@keio.jp*

[2]*Keio University, Yokohama, Japan, E-mail: ishigami@mech.keio.ac.jp*

ABSTRACT

Asteroid explorations are expected to reveal the origin of the solar system. One of the most critical phases on such explorations is the landing phase of the spacecraft since an impact force at the landing may damage the spacecraft. The impact force applied to the spacecraft has been estimated with model experiments or numerical simulations. However, the former requires an extremely small-scale model for a spacecraft landing on an asteroid with microgravity. As for numerical simulations, the validity of the contact dynamic model is still an open issue. This paper describes a landing dynamics analysis of the lander in the Martian Moons eXploration (MMX) mission as a target example. The analysis exploits a similarity law to correlate a lander dynamics with a model experiment. Since the gravitational acceleration of the Martian moon is much smaller than that of the Earth, the gravity term in the similarity law is explicitly considered. The experimental result clarifies that the impact force and landing velocity have a positive correlation with one another.

1 INTRODUCTION

Asteroid explorations are essential to obtain new information about the beginning of the solar system. One of the most critical phases on such explorations is the landing phase of the spacecraft, since a landing impact may overturn or damage the spacecraft. There have been two ways to estimate the impact force applied to the spacecraft: model experiments and numerical simulations.

The former was utilized in Apollo missions, and the behavior of the lunar lander was simulated with a 1/6-scale model [1]. The results being equivalent to those of full-scale tests conducted on the lunar-gravity simulator, in which the gravity of the Moon was realized by the landing on a slope. However, this approach requires an extremely small-scale model for a spacecraft landing on an asteroid with microgravity, which would make the experiments difficult.

On the other hand, numerical simulations have been applied to the asteroid spacecraft [2-4], while its contact dynamic model between the landing pad and an asteroid surface is still an open issue. In [5-7], the contact dynamic model was addressed through experimental methods at the gravity of the Earth. However, the relation between those experiments and the actual behavior of the lunar lander is unclear, and the impact force simulated in the experimental systems has not been validated yet.

This paper describes a landing dynamics analysis of the lander in the Martian Moons eXploration (MMX) mission [8] as a target example. The mission to be launched by JAXA aims to send a spacecraft towards the Martian moon and to land it on the surface of the Phobos, which is supposed to be covered with fine sand called regolith [9]. The analysis performed in this paper exploits a similarity law to correlate a lander dynamics with a model experiment. Since the gravitational acceleration of the Martian moon is much smaller than that of the Earth [10], the gravity term in the similarity law is explicitly considered when the model experiments are carried out to estimate the impact force.

The rest of this paper is organized as follows: Section 2 thoroughly follows the similarity law used in this research and derives key factors for the model experiment. Section 3 and 4 introduces the drop test setup and its results. Section 5 summarizes the findings from the research.

2 SIMILARITY LAW

In this research, first, similarity law will derive from the mechanical relations between the Earth and the Phobos.

In model experiments, the similarity law is generally established by correlating the phenomena observed in both practical and the model experiments. Then, quantitative relationships between the two phenomena are elaborated. The following method is known as the way to derive the similarity law based on laws of physics [11].

1. Observe the physical phenomena and select physical quantities assumed to be predominant in the phenomena.
2. Rewrite the selected quantities with physical values such as characteristic length.

Table 1: Dimensionless quantities.

Numerator / Denominator	① $\rho_p l^2 v^2$	② $\rho_r l^2 v^2$	③ $\rho_p g l^3$	④ $\rho_r g l^3$	⑤ cl^2
① Inertia force of the spacecraft: $\rho_p l^2 v^2$					
② Inertia force of the regolith: $\rho_r l^2 v^2$	$\frac{\rho_p}{\rho_r}$				
③ Gravitational force of the spacecraft: $\rho_p g l^3$	$\frac{v^2}{gl}$	$\frac{\rho_r}{\rho_p}\frac{v^2}{gl}$			
④ Gravitational force of the regolith: $\rho_r g l^3$	$\frac{\rho_p}{\rho_r}\frac{v^2}{gl}$	$\frac{v^2}{gl}$	$\frac{\rho_p}{\rho_r}$		
⑤ Cohesion force of the regolith: cl^2	$\frac{\rho_p v^2}{c}$	$\frac{\rho_r v^2}{c}$	$\frac{\rho_p gl}{c}$	$\frac{\rho_r gl}{c}$	

3. Calculate a ratio between the predominant quantities to derive the dimensionless quantities called pi.
4. Equalize the dimensionless quantities in the model experiment and in the real environment to derive the similarity law.

Here, the number of the dimensionless valuables assumed to be determined by the Buckingham Pi Theorem.

2.1 Assumption of the Predominant Physical Quantities

First, physical phenomena of the dynamical systems in which a spacecraft lands on a Martian moon are examined. The landing of the spacecraft can be physically described as the phenomenon in which the spacecraft moving with a certain velocity touches the surface of the Martian moon and reduces its velocity until it comes to rest. Here, since the spacecraft accelerates/decelerates, the inertia force applied to the spacecraft varies. Therefore, the inertia force of the spacecraft is one of the predominant physical quantities. In addition, the gravitational force of the spacecraft is important, because the spacecraft falls along in the direction of the gravity of the Martian moon. Also, when the spacecraft strikes against the surface of the Martian moon, the regolith, fine sand covering the surface, can be pushed down and compacted, or can be scattered. This means that the regolith initially staying on the surface moves owing to the landing, in other words, the regolith accelerates and the inertia force will be applied as well. The motion of the regolith can be influenced by the gravity of the Martian moon and the cohesion force of the regolith itself. Thus, the gravitational force and the cohesion force of the regolith should be also taken into account as the important phenomena during the landing process.

According to the above consideration, five physical quantities are assumed to be predominant when the spacecraft is landing on the Martian moon.

- Inertia force of the spacecraft: F_{ip}
- Inertia force of the regolith: F_{ir}
- Gravitational force of the spacecraft: F_{gp}
- Gravitational force of the regolith: F_{gr}
- Cohesion force of the regolith: F_c

2.2 Expression of Physical Quantities with Characteristic Values

In this section, the above five physical quantities are rewritten with the following characteristic values:

- Density of the spacecraft ρ_p
- Density of the reglith ρ_r
- Characteristic length: l
- Velocity: v
- Gravitational acceleration: g
- Cohesion stress of the regolith: c

These are the parameters that we need to deal with in the model experiments. They are also used to

determine the number of the dimensionless quantities in the Buckingham Pi Theorem explained in Section 2.5. The five predominant physical quantities can be rewritten with the characteristic vales as follows:

$$F_{ip} = m_p\alpha = \rho_p l^3(l/t^2) = \rho_p l^2 v^2 \quad (1)$$

$$F_{ir} = m_r\alpha = \rho_r l^3(l/t^2) = \rho_r l^2 v^2 \quad (2)$$

$$F_{gp} = m_p g = \rho_p g l^3 \quad (3)$$

$$F_{gr} = m_r g = \rho_r g l^3 \quad (4)$$

$$F_c = cl^2 \quad (5)$$

where m_p and m_r are the mass of the spacecraft and the regolith respectively, and t is the time.

The characteristic length represents the length of both the spacecraft and the regolith. However, if the diameter of the regolith grain were the characteristic length, the size of the regolith grain would need to be changed as the size of the spacecraft model varies, which would make the experiments extremely difficult. In order to solve such problems in the model experiments, the spatial accumulation effect is generally considered [11]. When we deal with the deformation of the soil, the motion of each grain is not considered, but physical quantities representing the macro properties such as the adhesive force. This research considers the spatial accumulation effect in order not to change the diameter of the regolith grain.

2.3 Selection of the Dimensionless Quantities

Table 1 shows all ratios generated from the relationship between the five predominant physical quantities defined in Eqs. 1-5. The ratio without cohesion force term can be written with two dimensionless quantities: the first quantity specified with the red circle in the table is the ratio of square of the velocity v to the product of the gravitational acceleration g and the characteristic length l. The other one enclosed in the green circle is the ratio of the density of the spacecraft to that of the regolith. If these two dimensionless quantities are selected as the pi numbers that the similarity law consists of, the relation between the gravitational forces and the inertia forces of the spacecraft and the regolith can be incorporated one another in the law. In addition to the two dimensionless quantities, the one enclosed in the yellow circle is selected as another pi that the similarity law consists of. The third pi is the ratio between the gravitational force and cohesion force of the regolith. The reason why this ratio is selected is that it defines the condition of the regolith, and that the similarity law in this research considers the gravitational force. Therefore, in order to derive the similarity law, the following dimensionless quantities should be considered:

$$\pi_1 \equiv \frac{F_{ip}}{F_{gp}} = \frac{F_{ir}}{F_{gr}} = \frac{v^2}{gl} \quad (6)$$

$$\pi_2 \equiv \frac{F_{gp}}{F_{gr}} = \frac{\rho_p}{\rho_r} \quad (7)$$

$$\pi_3 \equiv \frac{F_c}{F_{gr}} = \frac{\mathrm{c}}{\rho_r g l} \quad (8)$$

π_1 is the ratio of the inertia force to the gravitational force, and it is defined in the same way as the Froude number. π_2 is the ratio between the gravitational forces of the spacecraft and the regolith, and π_3 is the ratio between the gravitational force and cohesion force of the regolith. The validity of the number of the dimensionless quantities will be proven in the next section.

2.4 Buckingham Pi Theorem

The Buckingham Pi Theorem explains which variables can be reduced [12]:

If a physical process satisfies the principle of dimensional homogeneity and involves n dimensional variables, it can be reduced to a relation between only dimensionless variables. The reduction $j = n - k$ equals the maximum number of variables that do not form a pi among themselves and is always less than or equal to the number of dimensions describing the variables.

Given the above theorem to this research, first, the principle of dimensional homogeneity is satisfied because all the predominant physical properties assumed in Section 2.1 have the dimensions of the force. The number of the dimensional variables (the characteristic values) n is 6 as shown in Section 2.2.

Second, the dimension of each characteristic variables is examined. Here, the dimensions of mass, length, and time are defined as $\{M\}$, $\{L\}$, and $\{T\}$ respectively:

$$\{\rho_p\} = \{ML^{-3}\} \quad (9)$$

$$\{\rho_r\} = \{ML^{-3}\} \quad (10)$$

$$\{l\} = \{L\} \quad (11)$$

$$\{v\} = \{LT^{-1}\} \quad (12)$$

$$\{g\} = \{LT^{-2}\} \quad (13)$$

$$\{c\} = \{ML^{-1}T^{-2}\} \quad (14)$$

According to the above equations, all of the dimensional variables are described with $\{M\}$, $\{L\}$, and $\{T\}$. Then we derive

$$j = n - k \leq 3 \quad (15)$$

From Eq. 15, we obtain the constraint on the number of the dimensionless variables.

$$k = n - j \geq 6 - 3 = 3 \quad (16)$$

Eq. 16 is satisfied because the three dimensionless quantities differing from each other have been selected in the previous section. Therefore, the number of the dimensionless quantities we selected has proven to be valid.

2.5 Derivation of the Similarity Law

In this section, the similarity law will be derived. Given the superscript $'$ to the physical properties in the model experiment system, the dimensionless quantities in the model experiment and in the Martian moon environment are assumed to be equivalent to derive the following similarity law:

$$\pi_1 = \frac{v^2}{gl} = \frac{v'^2}{g'l'} \quad (17)$$

$$\pi_2 = \frac{\rho_p}{\rho_r} = \frac{\rho_p'}{\rho_r'} \quad (18)$$

$$\pi_3 = \frac{\mathrm{c}}{\rho_r g l} = \frac{\mathrm{c}'}{\rho_r' g' l'} \quad (19)$$

However, it would be difficult to realize the experimental system satisfying all of the three equations above, so we reduce the dimensionless quantities to relax the experimental conditions as Shimizu et al. reported in [13]. Firstly, π_2 is essential because it represents the relation between the gravitational forces of the spacecraft and of the regolith, which should be explicitly considered in this research. Secondly, π_1 and π_3 contain the inertia force and the cohesion force of the regolith respectively. As discussed in Section 2.1, the landing of the spacecraft were physically described as the phenomenon in which the spacecraft moving with a certain velocity touches the surface of the Martian moon and reduces its velocity until it comes to rest. Then the physical properties related to the velocity variation such as inertia force becomes important. It follows that π_1 should be considered. Therefore, the similarity law in this research is composed of Eqs. 17 and 18.

The similarity law should be transformed before it is applied to the experimental system in which the velocity of the model v' is realized through free fall test bench as described later. The velocity of the model v' can be rewritten with the drop height h'. Assuming that the spacecraft model of mass m_p' at rest reaches the velocity v' after falling freely from the height h', the law of conservation of the mechanical energy leads that

$$\frac{1}{2} m_p' v'^2 - m_p' g' h' = 0 \quad (20)$$

where g' denotes the gravitational acceleration of the Earth. Solving Eq. 20 for v', we obtain

$$v' = \sqrt{2g'h'} \quad (21)$$

Rewriting Eq. 17 with Eq. 21, we derive the similarity law modified for the drop tests as follows:

$$\pi_1 = \frac{v^2}{gl} = \frac{2h'}{l'} \quad (22)$$

$$\pi_2 = \frac{\rho_p}{\rho_r} = \frac{\rho_p'}{\rho_r'} \quad (23)$$

The model experiment setup follows the above similarity laws to estimate the landing behavior and impact force of the spacecraft.

3 DROP EXPERIMENT SETUP

3.1 Experimental Conditions based on Similarity Law

In this section, the conditions on the Phobos are applied to Eq. 22 to derive the maximum drop height of the model experiments. The gravitational acceleration of the Phobos is $g = 0.0057$ m/s^2 [10], and the maximum velocity of the spacecraft in MMX mission during the landing process is planed to be $v = 0.5$ m/s.

Here, the characteristic length l is a quantity used for obtaining the ratio between the sizes of the model and the real spacecraft. If the model has the same shape as the spacecraft, the length of any part can be selected as the characteristic length. However, our model copies the leg of the spacecraft, so we should define the length of one part as the characteristic length. This paper assumes that the spacecraft in the MMX mission lands with legs whose end has a circular plate called footpad. The footpads were used in previous landers such as Apollo missions shown in Figure 1 [14]. When the spacecraft has footpads, it can be assumed that the impact force applied to the spacecraft during the landing process depends on the contact area of the footpad. Therefore, we select the diameter of the footpad as the characteristic length. The diameter of

Figure 1: Footpad of Apollo 11.

the footpad of the MMX lander, which has not been determined yet, is assumed to be 0.3 m. Then the characteristic length of the real spacecraft is $l = 0.3$ m.

All the terms of the Martian moon environment in Eq. 22 has been determined, so those of the model experiments will be determined next. The model would be easy to handle when its diameter is dozens of millimeters. The ratio between the characteristic lengths of the model and the real spacecraft is assumed as

$$\frac{l'}{l} \approx \frac{1}{10} \tag{24}$$

Substituting Eq. 24 and $v = 0.5$ m/s into Eq. 22, we obtain

$$h' \approx 2.2 \text{ m} \tag{25}$$

Therefore, the model should drop from a height of 2.2 m to estimate the impact force applied to the spacecraft whose velocity is 0.5 m/s.

3.2 Experimental Setup

This section describes the drop experiment setup for the model experiments based on the similarity law. Figure 2 shows the overview of the setup. The model of the spacecraft falls freely to sand, and the displacement and acceleration of the model are measured with sensors.

In this setup, the spacecraft model moves in the vertical direction along the 1.8-meter-long linear motion guide. The vertical displacement of the model is measured with the laser displacement sensor (IL-2000; Keyence) with the resolution of 0.1 mm.

Figure 3 shows the schematic view of the spacecraft model. The model includes the acceleration sensor (TSR PRO; DTS) and the test piece imitating the footpad. The test pieces are made of shock resistant material called ultra high molecular weight polyethylene. The model slides on the linear motion guide with the part called the block. The mass of the model can be varied with adding dummy weights. The electromagnet holds the model at an appropriate height before releasing it at an arbitrary timing.

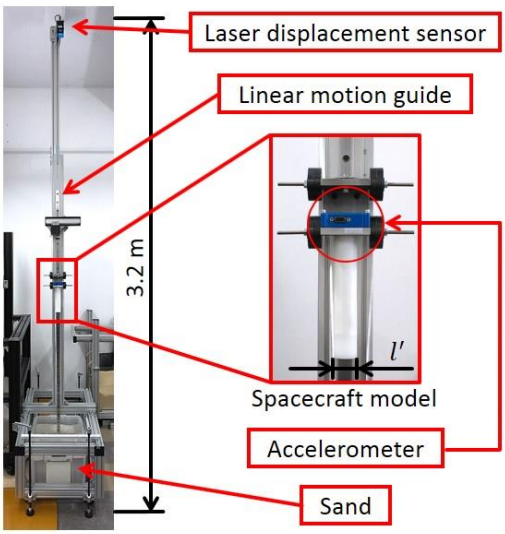

Figure 2: Overview of the drop experiment system.

4 DROP EXPERIMENTS

4.1 Density of the Model

This section describes the definition of the density and mass of the model. The density of the model ρ_p' satisfies the Eq. 23. This paper assumes that the regolith on the Phobos and the sand in the model experiment setup (Silica sand) have the same density:

$$\rho_r = \rho_r' \tag{26}$$

From Eq. 23, we get

$$\rho_p = \rho_p' \tag{27}$$

In addition, the density ρ has a unit of m/l^3, in which m is the mass, and l is the characteristic length. Then Eq. 27 can be rewritten with the mass of the spacecraft and the model.

$$m_p/l^3 = m_p'/l'^3 \tag{28}$$

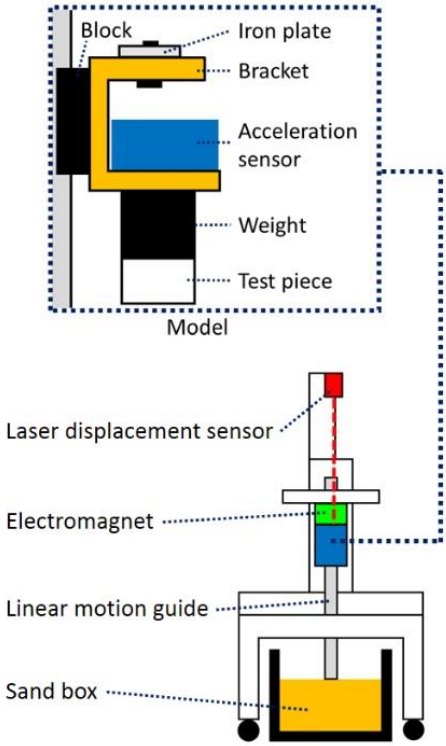

Figure 3: Schematic view of the drop experiment system.

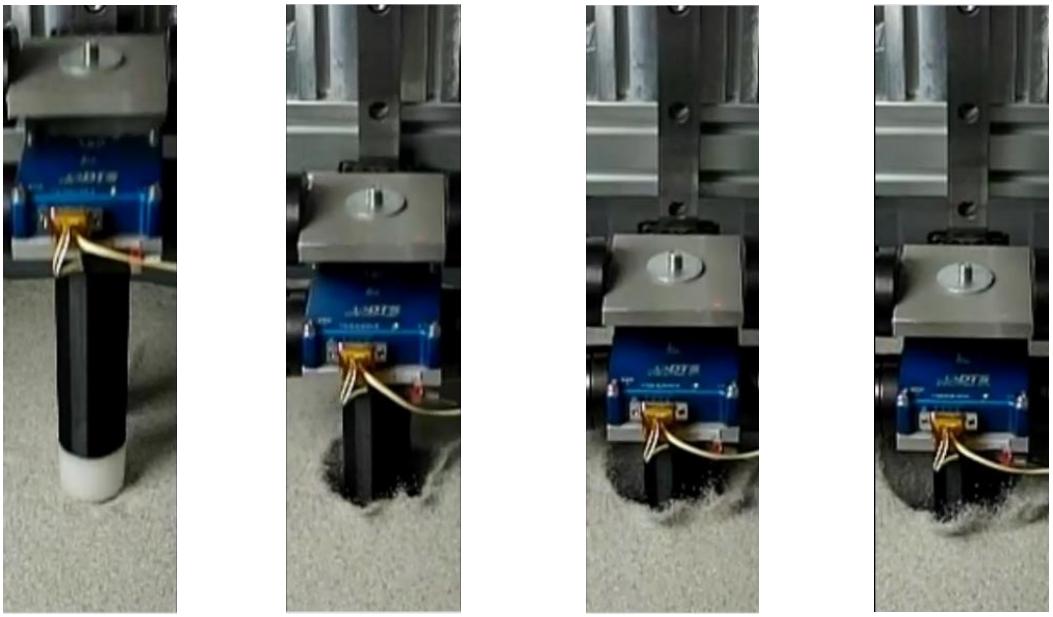

t = 0 ms t = 20 ms t = 40 ms t = 60 ms

Figure 4: Snapshots of a drop test ($l' = 40$ mm, $v = 0.3$ m/s).

Table 2: Experimental conditions.

(a) Assumptions about the spacecraft

Characteristic length l	300 mm
Mass m_p	1500 kg
Velocity v	0.10-0.35 m/s

(b) Conditions of the spacecraft model

Characteristic length l' [mm]	30	35	40
Mass m_p' [kg]	1.5	2.4	3.6

The above equation means that the mass of the model m_p' is calculated with the mass of the real spacecraft m_p and the ratio between the characteristic lengths l'/l. The mass of the MMX lander is supposed to be 1500 kg. We assume that all the impact force is applied to one footpad.

4.2 Drop Test

The drop tests were performed with three models of the spacecraft. Table 2 shows the assumptions about the real spacecraft and the conditions of the models. At the beginning of the test, the model was held at the height of h' in Eq. 22. Second, the laser displacement sensor, the acceleration sensor, and a high-speed camera start the data acquisition before the model of the spacecraft drops. Sampling rates of the laser displacement sensor and the acceleration sensor were 0.33 ms and 0.05 ms respectively. The high-speed camera (EX-F1; CASIO), whose frame rate was 1200 fps, records the behavior of the model and the sand. Figure 4 shows the behavior of a model ($l' = 40$ mm, $v = 0.3$ m/s) after striking the sand. The model sank while scattering the sand. Figure 5 shows the time variation of the acceleration of the model, which contacted the surface of the sand at $t = 0$ ms. The maximum acceleration emphasized with the red point in Figure 5 was defined as the impact acceleration of the model α'.

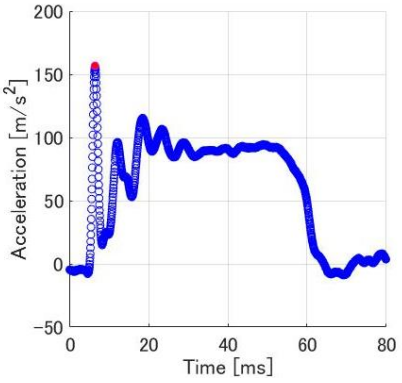

Figure 5: Acceleration-time

4.3 Similarity of the Experimental System

Before estimating the impact force applied to the spacecraft, the similarity law developed in this paper should be experimentally examined from the drop tests of models having different characteristic lengths. A new dimensionless quantity that includes the sinkage of the spacecraft will be introduced to check whether the sinkages of the models are similar or not.

First, assuming that the regolith can be modeled as a spring during the landing process, the following

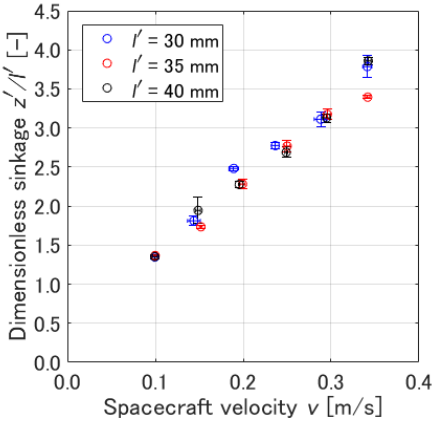

Figure 6: Dimensionless sinkage w.r.t. spacecraft velocity.

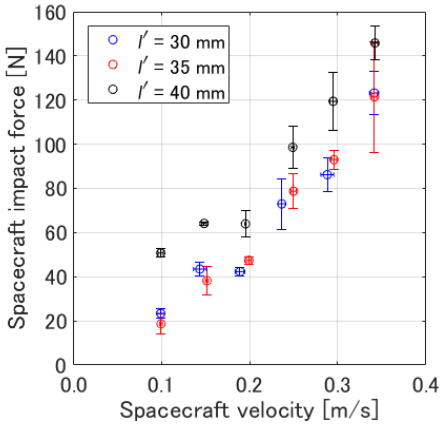

Figure 7: Spacecraft impact force w.r.t. spacecraft velocity.

force would be assumed to be applied to the sand:

$$F_{er} = kz = \rho_r l v^2 z \tag{29}$$

where z means the sinkage of the spacecraft, and k denotes the spring constant of the regolith, which can be rewritten with the characteristic values mentioned in Section 2.2. The force given by Eq. 29 is considered the elastic force of the regolith.

Second, a new dimensionless quantity concerning the sinkage of the spacecraft will be introduced. The ratio of the resistance of the regolith to the inertia force of the regolith in Eq. 2 becomes the dimensionless sinkage as follows:

$$\pi_s \equiv \frac{F_{er}}{F_{ir}} = \frac{\rho_r l v^2 z}{\rho_r l^2 v^2} = \frac{z}{l} \tag{30}$$

This dimensionless quantity should be constant in the drop tests under the same assumptions about the real spacecraft, because the tests are supposed to be similar with each other.

Figure 6 shows the dimensionless sinkage of the model z'/l' with regard to the spacecraft velocity. All the plots with the same velocity are in good agreement with each other, which demonstrates the similarity in the drop tests.

In addition, the sinkage seems to be a linear function of the spacecraft velocity as seen in Figure 6. This linearity can be explained by introducing the dimensionless energy. The ratio of the elastic potential energy of the regolith E_{er} to the kinetic energy of the spacecraft E_{kr} is

$$\pi_E \equiv \frac{E_{er}}{E_{kr}} = \frac{\frac{1}{2}kz^2}{\frac{1}{2}\rho_r l^3 v^2} = K\left(\frac{z}{v}\right)^2 \tag{31}$$

where K is a constant determined with the experimental conditions.

$$K = \frac{k}{\rho_r l^3} \tag{32}$$

When the dimensionless energy given by Eq. 31 is constant in the experimental system, we obtain

$$\frac{z}{v} = \text{constant} \tag{33}$$

The above equation means that the sinkage of the spacecraft z is proportional to the velocity v. Therefore, the slope on the graph in Figure 6 can be explained by the constant dimensionless energy in the experimental system. However, strictly speaking, the dimensionless sinkage of the model z'/l' is not proportional to the velocity v in Figure 6. The intercept provides the dimensionless sinkage when the velocity of the spacecraft is zero. In terms of energy, the intercept also gives the gravitational potential energy that the model has on the surface of the sand. From the above consideration, we suggest that the sinkage of the spacecraft should be predicted with the following equation:

$$\frac{z}{l} = \beta v + \gamma \tag{34}$$

where l is the characteristic length of the spacecraft, β is the constant which depends on the conditions of the regolith and the spacecraft, and γ is the constant concerning the gravitational potential energy of the spacecraft.

4.4 Estimation of the Impact Force

The similarity of the experimental system has been demonstrated in the previous section, so another dimensionless quantity would be introduced to estimate the impact force applied to the spacecraft. This research defines the impact force as follows:

$$F_{ap} = m_p \alpha = \rho_p l^3 \alpha \tag{35}$$

where α is the impact acceleration described in Section 4.2. The ratio between the impact force and

gravitational force of the spacecraft becomes:

$$\pi_a \equiv \frac{F_{ap}}{F_{gp}} = \frac{\rho_p \alpha l^3}{\rho_p g l^3} = \frac{\alpha}{g} \quad (36)$$

When the above dimensionless quantity is equal both in the experimental system on the Earth and in the environment of the Phobos, the impact force applied to the spacecraft is given as follows:

$$\alpha = \alpha' \frac{g}{g'} \quad (37)$$

where α' denotes the impact force applied to the model. Figure 7 shows the relationship between the impact force and velocity of the spacecraft. The result clarifies that the impact force $m_p \alpha$ and landing velocity has a positive correlation with one another. At $v = 0.3$ m/s, the impact force reaches 100 N, which is approximately 12 times as large as the gravitational force of the spacecraft on the Phobos.

5 CONCLUSION

The model experiments based on the similarity law were performed to estimate the landing impact applied to the Martian moon spacecraft. The physical phenomena during the landing process were carefully examined in order to select predominant physical properties. The similarity law can be derived when the dimensionless quantities given from two of the physical properties are equivalent between the experimental system and the real environment. The landing experiments using the drop test bench were performed with landing pad models having varied characteristic lengths. The similarity of the experimental system was verified with the dimensionless sinkage, which would be useful for predicting the sinkage of the real spacecraft. The impact force applied to the spacecraft was also predicted: the impact force has a positive correlation with the landing velocity. Our method can be applied to other asteroids or planets that have different gravity from the Earth.

In a future work, our model experiments are being compared with those performed in vacuum and microgravity environment to validate the method.

Acknowledgement

The authors acknowledge the support of Mr. K. Yamada, Mr. S. Hidaka, Mr. S. Horiko, Mr. R. Yoneyama, and Ms. H. Katsumata, who assisted the model experiments.

References

[1] Blanchard UJ (1968) Evaluation of a Full-scale Lunar-gravity Simulator by Comparison of Landing-impact Tests of a Full-scale and a 1/6-scale Model. *NASA Technical Note*, pp. 3-48.

[2] Kubota T, Otsuki M, Hashimoto T (2008) Touchdown Dynamics for Sample Collection in Hayabusa Mission. In: *proceedings of 2008 IEEE international conference on Robotics and Automation*, Pasadena, California, pp. 161-163.

[3] Nohmi M and Miyahara A (2005) Modeling for Lunar Lander by Mechanical Dynamics Software. In: *proceedings of AIAA Modeling and Simulation Technologies Conference and Exhibit*, San Francisco, CA, USA, pp. 61-68.

[4] Liang D, Chai H, and Chen T (2011) Landing Dynamic Analysis for Landing Leg of Lunar Lander using Abaqus/explicit. In: *proceedings of 2011 International Conference on Electronic & Mechanical Engineering and Information Technology*, Heilongjiang, China, pp. 4364-4367.

[5] Sutoh M, Wakabayashi S, and Hoshino T (2017) Motion Behaviors of Landing Gear for Lunar Probe in the Atmosphere and Vacuum. *IEEE Robotics and Automation Letters* 2(1): 313-320.

[6] Huang B, Jiang Z, Lin P, and Ling D (2015) Research on Impact Process of Lander Footpad against Simulant Lunar Soils *Shock Vibration* Vol. 2015, Art. no. 658386, pp. 1-25.

[7] Yokoyama T, Kanamori H, and Higuchi K (2006) Estimate of Impact Force at Landing on Lunar Surface with Scale Model Experiment *Paper presented at 5th International Symposium on Scale Modeling*, Chiba, Japan, Sep. 2006.

[8] JAXA. MMX - Martian Moons eXploration. Available at: http://mmx.isas.jaxa.jp/en/

[9] Busch MW, Ostro SJ, Benner LAM, Giorgini JD, Magri C, Howell ES, Nolan MC, Hine AA, Campbell DB, Shapiro II, and Chandler JF (2007) Arecibo radar observations of Phobos and Deimos *ICARUS* 186: 581-584.

[10] NASA. Phobos by the Numbers–Solar System Exploration. Available at: https://solarsystem.nasa.gov/moons/mars-moons/phobos/by-the-numbers/

[11] Emori I, Sekimoto K, and Saito K (2000) *Theory and Application of the Model Experiments*. Tokyo, Japan: Gihodo Shuppan, pp. 33-57. Japanese.

[12] White FM (2011) *Fluid Mechanics*. Singapore: McGraw-Hill, p. 311.

[13]Shimizu S (2007) *Analysis on Landing Dynamics of a Lunar Probe based on Scale Model Experiments*. Master Thesis, Tohoku University, Sendai, Japan. Japanese.

[14] NASA. Apollo 11 Image Gallery. Available at: https://history.nasa.gov/ap11ann/kippsphotos/apollo.html